



EUROfusion

WPS1-CPR(17) 17420

N Krawczyk et al.

Electron temperature estimation using the Pulse Height Analysis System at Wendelstein 7-X Stellarator

Preprint of Paper to be submitted for publication in Proceeding of
13th International Symposium on Fusion Nuclear Technology
(ISFNT)



This work has been carried out within the framework of the EUROfusion Consortium and has received funding from the Euratom research and training programme 2014-2018 under grant agreement No 633053. The views and opinions expressed herein do not necessarily reflect those of the European Commission.

This document is intended for publication in the open literature. It is made available on the clear understanding that it may not be further circulated and extracts or references may not be published prior to publication of the original when applicable, or without the consent of the Publications Officer, EUROfusion Programme Management Unit, Culham Science Centre, Abingdon, Oxon, OX14 3DB, UK or e-mail Publications.Officer@euro-fusion.org

Enquiries about Copyright and reproduction should be addressed to the Publications Officer, EUROfusion Programme Management Unit, Culham Science Centre, Abingdon, Oxon, OX14 3DB, UK or e-mail Publications.Officer@euro-fusion.org

The contents of this preprint and all other EUROfusion Preprints, Reports and Conference Papers are available to view online free at <http://www.euro-fusionscipub.org>. This site has full search facilities and e-mail alert options. In the JET specific papers the diagrams contained within the PDFs on this site are hyperlinked

Electron temperature estimation using the Pulse Height Analysis System at Wendelstein 7-X stellarator

Natalia Krawczyk^{*a}, Monika Kubkowska^a, Agata Czarnecka^a, Sławomir Jablonski^a, Marta Gruca^a, Tomasz Fornal^a, Leszek Ryc^a, Henning Thomsen^b, Golo Fuchert^b and W7-X team^b

^a*Institute of Plasma Physics and Laser Microfusion, Hery 23 St. 01-497 Warsaw, Poland*

^b*Max-Planck-Institut für Plasmaphysik, Wendelsteinstrasse 1, 17491 Greifswald, Germany*

This paper presents measurements of the electron temperature in Wendelstein 7-X (W7-X) stellarator plasmas heated by electron-cyclotron-resonance (ECRH) during the first operational phase (OP1.1). The analysis of the slope of the observed X-ray continuum emission (in a semi-logarithmic plot) measured by the use of the Pulse Height Analysis (PHA) system, provides the information about the electron temperature (T_e) of the hydrogen plasma. The determination of this fundamental plasma parameter is based on the exponential dependence of the continuum radiation (Bremsstrahlung) on photon energy assuming Maxwellian distribution. In this paper, some experimental results of the estimated electron temperature are presented and compared to the results obtained from the simulations of X-ray spectrum and other diagnostic like the Thomson Scattering (TS) system.

Keywords: PHA diagnostic, electron temperature, stellarator, Wendelstein 7-X

1. Introduction

Wendelstein 7-X (W7-X) [1-2], a large optimized stellarator with superconducting coil system started its first operational phase (OP1.1) at the end of 2015. For OP1.1, the last closed flux surface (LFCS) was defined by five poloidal uncooled limiters made of graphite. The brief experimental campaign allowed the commissioning of installed diagnostic systems and W7-X components as well as the initial physics studies [3-5].

Electron temperature (T_e) as a one of the key plasma parameters, which indicate fusion performance, was routinely measured during the W7-X experiments. In the OP1.1 limiter configuration electron temperatures $T_e \leq 8$ keV have been achieved. The major tools for the T_e determination at W7-X are Thomson scattering (TS) [6] and Electron Cyclotron Emissions (ECE) [7] diagnostics. Both systems, which are capable to provide electron temperature profiles, have confirmed good agreement between their results throughout OP1.1 [8].

Measurements of T_e can be also performed by the Pulse Height Analysis (PHA) [9-12] system installed at W7-X, which primary purpose is impurity content estimation [13-14] and additionally characterization of nonthermal features of the plasma spectral emission [15]. The PHA spectra provide information about line-averaged electron temperature ($\langle T_e \rangle$), as an average along the line-of-sight, as opposed to measurements from TS and ECE diagnostics. For the investigation described in this paper, a set of data has been selected to demonstrate the system capability to measure $\langle T_e \rangle$.

2. Experimental setup of the PHA system

The PHA system commissioned and tested during OP1.1 [16] was designed to provide spectra in the range from 0.7 keV up to 19 keV (for 1/e of detector response). It consists of 3 Silicon Drift Detectors (SDD) equipped with individual square pinholes and additional exchangeable Be filters of various thickness, to reduce the number of photon flux that reach the detectors. The first two detectors with a thickness of 450 μm and an active area of 10 mm^2 are equipped with an 8- μm Beryllium window, while the third one is characterized by a very thin polymer window. For the presented analysis, data in the range from 0.9 keV up to 10 keV (due to the MCA (multi-channel analyzer) settings) have been considered. The PHA energy resolution is better than 200 eV to resolve the impurities spectral lines. The time resolution is 100 ms and the spatial resolution, for pinhole size equal to 300 \times 300 μm^2 , is 2.5 cm.

For $\langle T_e \rangle$ estimation described in this paper the 1st PHA channel (with additional 25 μm of Be filter) signals obtained for the trigger threshold of 1000 eV, the peaking time of 1 μs and the pinhole size of 300 \times 300 μm^2 were employed. This was because, during the OP1.1 only 1st PHA channel has been optimized to minimize pileup effect. In Fig.1 the line-of-sight (LOS) of detector 1 is shown. The LOS simulation, which is based on flux surface data (VIMEC) from magnetic configuration J (used during OP1.1), shows that the mentioned detector should view almost (about 8,5 cm) through the plasma center.

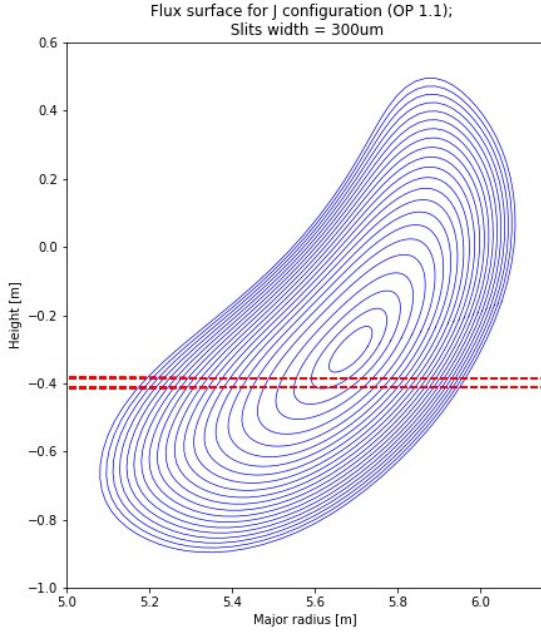


Fig. 1. Flux surfaces (blue) in the poloidal plane with the line-of-sight (red) observed by PHA Channel 1. Flux surfaces taken from VMEC calculation for W7-X program #20160309.025.

3. Determination of the electron temperature from the PHA spectra – theoretical description

The soft X-ray radiation from plasmas, is composed of free-free (Bremsstrahlung), free-bound (recombination radiation) and bound-bound (line radiation) emissions. The first two types of radiation form a continuum spectrum. The equation for hydrogenic bremsstrahlung plasma is as follows [15]:

$$\left(\frac{dP_{ff}}{dVdE} \right)_{ff} = 3 \cdot 10^{-15} n_e \sum_i n_i Z_i^2 T_e^{-\frac{1}{2}} g_{ff} e^{-\frac{E}{k_b T_e}} \quad (1)$$

where dP_{ff} [W] is the power radiated by an impurity ion with the ion charge Z_i and ion density n_i per unit volume dV [m^3] as well as the energy interval dE [eV]. T_e [eV], n_e and E [eV] are the electron temperature, electron density and photon energy, respectively. g_{ff} is the Maxwell-averaged Gaunt factor, which is approximately equal 1 in most cases.

As in the free-bound case the radiation intensity is given by [15]:

$$\left(\frac{dP_{fb}}{dVdE} \right)_{fb} = 3 \cdot 10^{-15} n_e \sum_i n_i Z_i^2 T_e^{-\frac{1}{2}} g_{fb} e^{-\frac{E}{k_b T_e}} \beta \quad (2)$$

$$\beta = \frac{\xi}{n_0^3} \frac{\chi_{Z-1}^{n_0}}{T_e} e^{-\frac{\chi_{Z-1}^{n_0}}{k_b T_e}} + \sum_{n>n_0} \frac{2}{n^3} \frac{\chi_{Z-1}^{n_0}}{T_e} e^{-\frac{Z^2 \chi_H}{n^2 k_b T_e}}$$

Here, continuum radiation is due to the radiative recombination of ions with charge Z_i to Z_i-1 . χ_H is the ionization potential of hydrogen, χ_i is the ground state ionization potential and n is ground state principal quantum number.

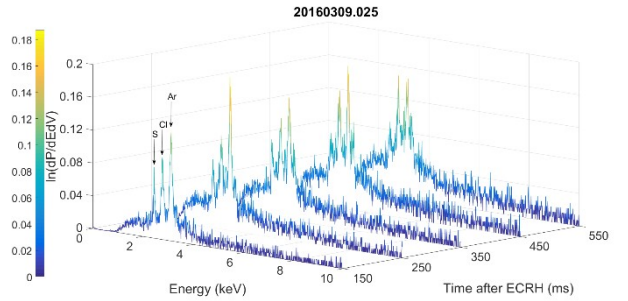
The principle of electron temperature determination from the continuum [11-12], is based on the exponential dependence describing bremsstrahlung radiation (eq.1). On the assumption that g_{ff} is independent of energy, T_e is directly calculated from the slope ($a = \frac{-1}{T_e}$) of a straight line fitted to the continuum radiation (in a semi-logarithmic plot of $dP_{ff}/dVdE$ vs Energy)

Additionally, the results obtained from experimental spectra are compared with the T_e from simulations to see if they agreed. In order to simulate the X-ray spectra (the continuum radiation in this particular case), a numerical code RayX was used [17]. It was based on coronal equilibrium of hydrogen plasma and it assumed that each part of the observed plasma volume gives appropriate contribution to the final spectrum. The profiles of the electron temperature $T_e(r)$ and density $n_e(r)$ for specific time frames are taken from Thomson Scattering diagnostic.

4. Experimental results

The results of the electron temperature estimation from PHA data presented in this section were obtained from the plasma discharge #20160309.025. This experiment featured a hydrogen plasma with argon tracer impurities for diagnostic purposes and ECRH heating at a stable level of 2 MW. The discharge duration was 700 ms.

(a)



(b)

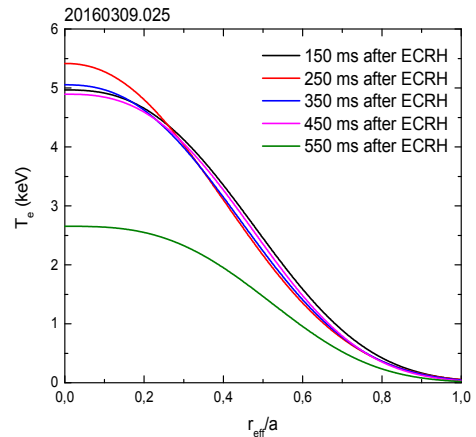


Fig.2. (a) Spectra at particular time frames for W7-X program #20160309.025 collected by PHA channel 1 and (b) corresponding $T_e(r)$ profiles provided by Thomson Scattering system

For this analysis, five time frames with PHA spectra have been used (cf. Fig 2). Each of them contains data from a 100 ms time interval. The first frame shows the data recorded 150 ms after ECRH start, while the last time frame is taken after 550 ms. In Figure 3, the spectra from the selected time frames are presented. In figure 2(b) the corresponding $T_e(r)$ profiles measured by Thomson scattering diagnostic (TS) are shown. The experimental points were fitted with the use of equation:

$$T_e(r) = T_{e0} \left[1 - \left(\frac{r}{a} \right)^m \right]^n \quad (3)$$

where T_{e0} is the central electron temperature, r is the effective radius, a is the minor radius, which was defined by the limiters in OP1.1 to ~ 0.49 m (in r_{eff}) and m, n are interpolation coefficients.

The choice of these particular time frames was dependent on two major factors. First, the quality of data provided by the PHA system needs to have feasible statistics (above ~ 10 000 counts, no pile-up effects) which allows to observe clear continuum radiation. Second, the profiles of the electron temperature $T_{e(r)}$ and density $n_{e(r)}$ required for simulation should be satisfactory (physically acceptable). The procedure of estimation the electron temperature $\langle T_e \rangle$ is illustrated in Fig.3 on the example of the frame number 2 (250 ms after ECRH start).

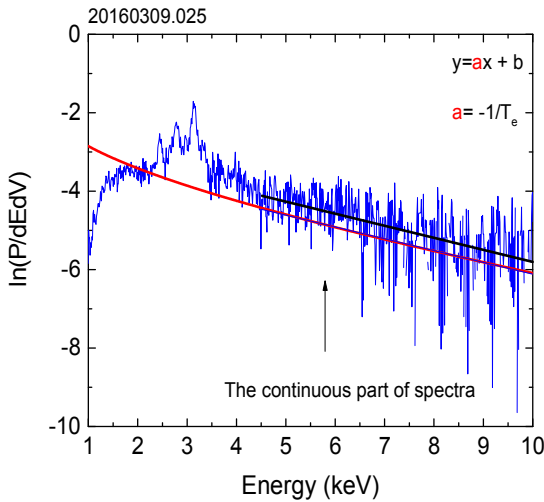


Fig. 3. Determination of the electron temperature from the slope of continuum radiation – on the basis of the PHA spectra (blue) and simulated one from RayX code (red).

In a semi-logarithmic plot of X-ray radiated power emission into energy interval and volume as a function of energy, the PHA spectrum (blue line) and simulated continuum radiation (red line) are presented. For both cases, experimental and simulated data, straight lines were fitted to the bremsstrahlung (using the method of least squares) in the energy range between 4.5 keV and 10 keV.

This energy range was chosen because it is free of line radiation, as well as, has enough number of counts. For this specific frame 250 ms after ECRH start, $T_{e(r)}$ and $n_{e(r)}$ profiles (from a fit to the TS data, cf. Fig 2b) used in simulation have a central electron temperature $T_{e0} = 5.4$ keV and central electron density $n_{e0} = 1.92 \times 10^{19} \text{ 1/m}^3$ (both values are taken from Thomson measurements). As result, the average temperature estimated from the slope of the simulated continuum, is $\langle T_{e,\text{sim}} \rangle = (3.320 \pm 0.004)$ keV. on the result from the experimental PHA spectrum is $\langle T_{e,\text{exp}} \rangle = (3.22 \pm 0.22)$ keV. These values show good agreement between simulation based on TS data and PHA data analysis within the error bars. It could be achieved due to sufficient quality of the data from the PHA and TS systems. In the Tab.1, results for all five time frames of the pulse #20160309.025 are shown. The values of $\langle T_e \rangle$ estimated from both analyzes are very similar, especially for frames 2 and 3. The biggest differences between the obtained results appear, when the PHA spectra recorded a small number counts which leads to higher uncertainties in bremsstrahlung (frame 1) or $T_{e(r)}$ and $n_{e(r)}$ profiles. Also for frame 5, there is a discrepancy between experimental and simulation data. This may be caused by a slight delay of PHA time frames during OP1.1. Both, in $\langle T_e \rangle$ from PHA spectra and simulations based on TS profiles, the errors were calculated as standard deviation of the line fitted to the Bremsstrahlung, due to the fact that the main source of errors in presented discharges is the statistics of the recorded counts.

Table 1. Comparison of the electron temperature estimated from the PHA spectra and simulations for discharge #20160309.025

Time after ECRH start (ms)	$\langle T_e \rangle$ from PHA spectra (keV)	$\langle T_e \rangle$ from simulations (keV) based on TS profiles
150 (frame1)	3.75 ± 0.72	3.180 ± 0.003
250 (frame2)	3.22 ± 0.22	3.320 ± 0.004
350 (frame3)	3.25 ± 0.24	3.230 ± 0.004
450 (frame4)	3.53 ± 0.25	3.210 ± 0.004
550 (frame5)	3.55 ± 0.22	2.050 ± 0.002

Although, the PHA system is set to observe across the plasma center, $\langle T_e \rangle$ values determined from experimental data are always lower than the central electron temperatures provided by the TS system (see $T_e(r_{\text{eff}}=0)$ in fig.2b). This could be explained by the fact that the measurement from the soft X-ray diagnostic is averaged over plasma plasma regions with different temperatures along the line-of-sight.

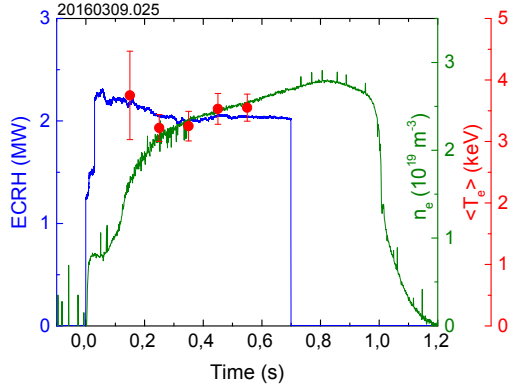


Fig. 4. The average electron temperature $\langle T_e \rangle$ estimated from the PHA spectra in comparison with ECRH heating and electron density

Moreover, on the basis of the presented pulse, $\langle T_e \rangle$ estimated from experimental spectra remains stable during the ECRH heating, which was set at an almost constant level of power (~ 2 MW during 700 ms). This typical trend is presented in Fig.4. Additionally, Fig.5 presents experimental results from PHA and TS systems including data from discharge #20160309.024 with different ECRH steps (from ~ 0.6 MW to 2 MW). In this particular case, the maximum difference between $\langle T_e \rangle$ (from PHA diagnostic) for the lowest and highest ECRH step is around 1 keV, although the heating power was increased by a factor of 4.

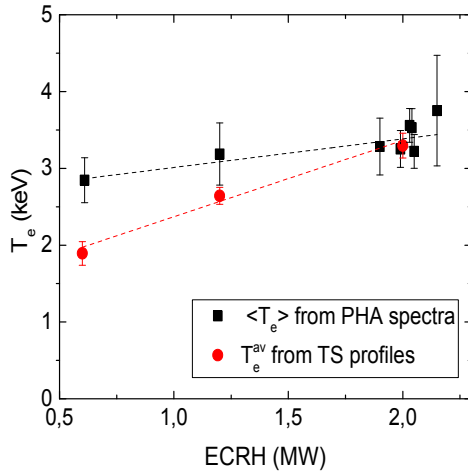


Fig. 5. The change of $\langle T_e \rangle$ with ECRH power for experimental data from discharges #20160309.024 and #20160309.035

A comparable trend was observed for the data obtained by the TS system. Here, the difference between averaged T_e^{av} is calculated using the following formula:

$$T_a^{av} = \frac{\int_0^r T_e(r) n_e(r) dr}{\int_0^r n_e(r) dr} \quad (4).$$

The maximum difference was $T_{e,max}^{av} = 1.4$ keV, which is consistent with the experimental PHA results.

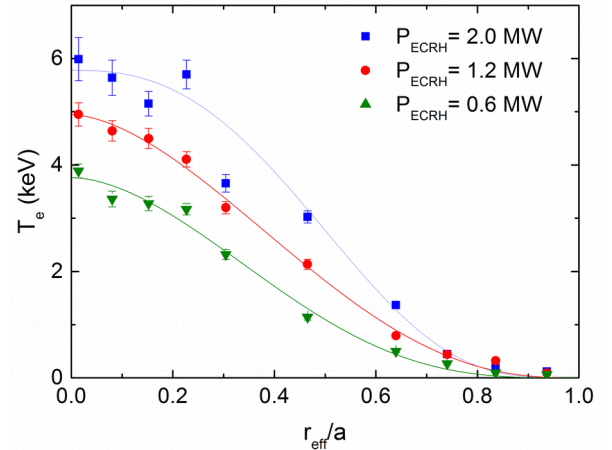


Fig. 6. $T_e(r)$ profiles based on measurements provided by Thomson Scattering system from discharge #20160309.024 with three different ECRH steps.

In Fig.6, The temperature profiles from Thomson scattering for the three ECRH steps are shown.

The slight difference between results obtained by the PHA and TS systems, respectively, could be explained by the fact that TS collects data directly through the plasma center, while the LOS of the 1st PHA channel system is located around 8.5 cm below the plasma center (according to VMEC equilibrium reconstructions of the flux surfaces). In order to understand the small responsiveness of the average temperature to the provided heating power, more detailed analysis of the temperature and density profiles are required, which is planned as a next step.

4. Conclusions

First results obtained by the PHA system during the OP1.1, confirmed its readiness to provide information about the plasma electron temperature. A correct estimation of T_e from the continuous part of the spectra was possible in all the cases, were collected spectra had sufficient counting statistic. Results obtained by analysis of the experimental data were consistent with those, which were derived from the simulated spectra. Moreover, very short acquisition time, which for the PHA system is equal to 100 ms, allows to observe even small changes of T_e during the discharge.

During the next experimental campaign of W7-X (OP1.2), a further optimization of the PHA system is planned. The aim is to measure spectra with higher number of counts and avoiding pile-up effects. As a result, it should be possible to determine $\langle T_e \rangle$ for most time frames during a typical W7-X pulse.

Acknowledgements

This work has been carried out within the framework of the EUROfusion Consortium and has received funding from the Euratom research and training programme 2014-2018 under grant agreement No 633053. The views and

opinions expressed herein do not necessarily reflect those of the European Commission.

This scientific work was partly supported by Polish Ministry of Science and Higher Education within the framework of the scientific financial resources in the years 2014-2017 allocated for the realization of the international co-financed project.

References

- [1] H.-S. Bosch et al., Technical challenges in the construction of the steady-state stellarator Wendelstein 7-X Nuclear Fusion 53 (2013) 126001
- [2] T. Sunn Pedersen et al., Plans for the first plasma operation of Wendelstein 7-X, Nuclear Fusion 55 (2015) 126001
- [3] R. Koenig et al., The Set of Diagnostics for the First Operation Campaign of the Wendelstein 7-X Stellarator, Journal of Instrumentation 10 (2015) P10002
- [4] T. Klinger et al., Performance and properties of the first plasmas of the Wendelstein 7-X Stellarator, Plasma Physics and Controlled Fusion (2016) 101221.R1
- [5] M. Krychowiak et al., Overview of diagnostic performance and results for the first operation phase in Wendelstein 7-X, Review of Scientific Instruments 87 (2016) 11D304
- [6] E. Pasch et al., The Thomson scattering system at Wendelstein 7-X Review of Scientific Instruments 87 (2016) 11E729
- [7] S. Schmuck et al., Design of the ECE diagnostic at Wendelstein 7-X, Fusion Engineering and Design 84 (2009)
- [8] E. Pasch et al., First results from the Thomson Scattering System at the Stellarator Wendelstein 7-X, 43rd EPD Conference on Plasma Physics
- [9] M. Kubkowska et al., Laboratory tests of the Pulse Height Analysis system for Wendelstein 7-X, Journal of Instrumentation 10 (2015) P10016
- [10] A. Weller et al., Concepts of X-ray diagnostic for Wendelstein 7-X, Review of Scientific Instruments 75,10 (2014)
- [11] A. Weller et al., X-ray Pulse Height Analysis on Asdex Upgrade, 38th EPS Conference on Plasma Physics (2011) P5.054
- [12] D. Pasini et al., JET X-ray pulse-height analysis system, Review of Scientific Instruments 59 (1988)
- [13] M. Kubkowska et al., First Results from the Soft X-ray Pulse Height Analysis System at Wendelstein 7-X Stellarator, 19th ISFNT, Kyoto, Japan 2017
- [14] A. Czarnecka et al., Study of impurities behaviour in PHA spectra for first magnetic configuration changes in W7-X plasmas, 19th ISFNT, Kyoto, Japan 2017
- [15] S. von Goeler et al., Thermal X-ray spectra and impurities in the ST Tokamak, Nuclear Fusion 15 (1975)
- [16] N. Krawczyk et al., Commissioning and first operation of the pulse-height analysis diagnostic on Wendelstein 7-X stellarator, Fusion Engineering and Design (2017)
- [17] S. Jablonski et al., Simulation of PHA Soft X-Ray Spectra expected from W7-X, Journal of Instrumentation 10 (2015)